FACTA UNIVERSITATIS
Series: **Mechanical Engineering** Vol. 17, N° 3, 2019, pp. 445 - 454
https://doi.org/10.22190/FUME190510040S

Original scientific paper

SURFACE MORPHOLOGY AND MICROHARDNESS BEHAVIOR OF 316L IN HAP-PMEDM

Gurpreet Singh[1], Yubraj Lamichhane[2], Amandeep Singh Bhui[2], Sarabjeet Singh Sidhu[1], Preetkanwal Singh Bains[1], Prabin Mukhiya[2]

[1]Mechanical Engineering Dept., Beant College of Engineering and Technology, India
[2]Mechanical Engineering Dept., Amritsar College of Engineering and Technology, India

Abstract. *The development of biomaterials for implants nowadays requires materials with superior mechanical and physical properties for enhanced osseointegration and sustained longevity. This research work was conducted to investigate the influence of nano hydroxyapatite (HAp) powder mixed electrical discharge machining (PMEDM) on surface morphology and microhardness of modified 316L stainless steel surface. The chosen process parameters were discharge current, pulse on/off duration and gap voltage in order to analyze the selected output responses. HAp concentration (15 g/l) along with reverse polarity was kept constant for current experimentation. The experimental results testified that surface morphology of PMEDM surface was significantly improved along with augmentation of 79% in microhardness (HV) of HAp modified surface of medical grade stainless steel. Furthermore, XRD and SEM characterization confirmed the deposition of calcium, phosphorous and inter-metallic compounds on HA-PMEDMed surface. The surface thus produced is expected to facilitate better bone-implant adhesion and bioactivity.*

Key Words: *PMEDM, 316L SS, Copper Tool, HAp Powder, Microhardness, Bioactivity*

1. INTRODUCTION

Biomaterials are artificial organs or implants preferably from the family of ceramics, polymeric and metallic biomaterials (titanium alloys, stainless steel 316L and Cr-Co alloys) for the substitution of the damaged human body organ. Prominent properties such as cell proliferation, bone-implant adhesion, osseointegration, corrosion and wear behavior in fluidic environment within the individual primarily affect the acceptance or rejection of the selected biomaterials [1, 2]. The demand for orthopedic implants is rising day by day; fascinating the researchers and engineers to improve its surface integrity alongside offering better resistance towards wear and corrosion [3-6]. As a result, implant surface must be modified with

Received May 10, 2019 / Accepted August 08, 2019
Corresponding author: Gurpreet Singh
Department of Mechanical Engineering, Beant College of Engineering & Technology, Gurdaspur – 143521, Punjab, India
E-mail: singh.gurpreet191@gmail.com

bioactive coating, avoiding the release of harmful ions causing corrosion and loosening of joint due to wear [7, 8]. Among all the established coating techniques, such as sol-gel, dip coating, ion implantation, PVD, CVD, laser coating, etc., the execution of EDM as an alternative to other surface modification methods is still in its beginning era [9].

In this method, bioactive powder is mixed in dielectric medium keeping workpiece as cathode (-) and tool electrode as anode (+) or simply negative polarity [10]. During the process, the produced thermal energy heated up the working area and with the flow of charge from positive to negative, the powder particles strike the surface and solidify in pulse-off duration and thus modify the substrate surface [11].

Different experimentations and techniques were explored by researchers in order to modify the surface characteristics of metallic biomaterials. Hubler et al. [12] studied wear and corrosion resistance of the 316L SS femoral implants by depositing the ceramics thin films of the transition metals nitrides and Ti/N and Cr/V layers. It was found that the coatings significantly improved the surface integrity, microhardness and corrosion resistance of the surface. Kumar et al. [13] investigated the electrochemical behavior and *in-vitro* bioactivity of polypyrrole/TiO_2 ceramic nano-composites on 316L stainless steel. It was found that addition of TiO_2 exhibits improved corrosion resistance properties of the substrate and offered better biocompatibility. Microhardness and *in-vitro* wear behavior of TiO_2 treated 316L stainless steel was examined by Singh et al. [14] *via* electro-discharge treatment. They found that material transfer rate of EDM is appropriate for the surface modification of bare metal. Addition of TiO_2 exhibits improved microhardness of 233% and protective efficiency of 80% compared to the substrate material. Chang et al. [15] inspected microhardness, corrosion resistance and protein adsorption properties of $CuAlO_2$ deposition on 316L stainless steel. With the use of nano-indentation, it was found that corrosion resistance and microhardness were significantly enhanced with an increment of 46% after the process.

Optimal ED machining parameters were investigated by Bhui et al. [16] for the surface modification of Ti6Al4V with graphite tool. Deposition of bioactive layer and formation of intermetallic compounds were examined using SEM and XRD respectively. Additionally, apatite growth was observed on machined sample confirming the bioactivity through SEM and EDS analysis. Harun et al. [17] in their study deeply reviewed the application of hydroxyapatite coatings for metallic biomaterials. It was found that hydroxyapatite powder dominantly improves the surface adhesion strength, biocompatibility and corrosion resistance of the metallic biomaterials [18-20].

Based on the literature survey and previous studies, it was seen that the use of EDM for modifying the biomaterials surface is still in its early stages [21, 22]. As there is no need for vacuum chamber or any special arrangement, the use of ED machining for the surface modification is a better choice when compared to other pricy techniques [23-25]. In the present study, stainless steel 316L; a well-known dominating biomaterial in the field of orthopaedics and joint replacement was investigated for modified surface integrities and microhardness in hydroxyapatite (HAp) powder mixed EDM with copper tool.

2. EXPERIMENTAL WORK

2.1. Materials

Metallic biomaterial 316L stainless steel was procured as workpiece material for the current experimentation having thermal conductivity 21.5 W/m.k at 500 °C; melting point 1371-1399 °C; and density 7.99 g/cc. Tables 1 and 2 show the elemental composition of 316L SS and hydroxyapatite powder, respectively. A pure copper circular electrode (of 10mm

in diameter) was used to machine the workpiece, whereas the HAp was in nano-size with true density 3.219 g/cm^3 and average particle size of 20-45 nm.

Table 1 Chemical composition of 316L SS

Element	Si	C	Mn	N	P	Cr	Ni	Mo	S	Fe
%	0.41	0.01	1.07	0.10	0.02	16.13	10.15	2.05	0.01	Balance

Table 2 Composition of hydroxyapatite powder

Element	$Ca_5(OH)(PO_4)_3$	Al_2O_3	Fe_2O_3
%	>99.5	<0.06	<0.02

2.2. Method

Design of experiments (DOE) was generated according to Taguchi's L_{18} orthogonal array employing mixed level design ($2^1 \times 3^4$) with the help of Minitab-17. Five machining parameters, i.e. dielectric medium (Dm), current (Ip), pulse-on time (P-on), pulse-off time (P-off) and voltage (V), were chosen to vary at three levels (Table 3) for the output responses.

Based on the levels of input parameters and experimental design, each experiment was performed on two different plates and an average of both is plotted for the result analysis. Machining time of 30 minutes and reverse polarity were kept constant throughout the experimentation. The following Table 4 illustrates the experimental design based on L_{18} orthogonal array.

Table 3 Input machining parameters

Input parameters (Symbol)	Units	Level 1 (low)	Level 2 (medium)	Level 3 (high)
Dielectric medium (Dm)	-	Hydrocarbon oil	Hydrocarbon oil + HAp	-
Current (Ip)	A	20	24	28
Pulse-on time (P-on)	µs	60	90	120
Pulse-off time (P-off)	µs	60	90	120
Voltage(V)	V	40	60	80

Table 4 Experimental design according on L_{18} orthogonal array

Exp. Run	Dielectric medium (Dm)	Current (Ip)	Pulse-on time (P-on)	Pulse-off time (P-off)	Voltage (V)
1	Hydrocarbon oil	20	60	60	40
2	Hydrocarbon oil	20	90	90	60
3	Hydrocarbon oil	20	120	120	80
4	Hydrocarbon oil	24	60	60	60
5	Hydrocarbon oil	24	90	90	80
6	Hydrocarbon oil	24	120	120	40
7	Hydrocarbon oil	28	60	90	40
8	Hydrocarbon oil	28	90	120	60
9	Hydrocarbon oil	28	120	60	80
10	Hydrocarbon oil + HAp	20	60	120	80
11	Hydrocarbon oil + HAp	20	90	60	40
12	Hydrocarbon oil + HAp	20	120	90	60
13	Hydrocarbon oil + HAp	24	60	90	80
14	Hydrocarbon oil + HAp	24	90	120	40
15	Hydrocarbon oil + HAp	24	120	60	60
16	Hydrocarbon oil + HAp	28	60	120	60
17	Hydrocarbon oil + HAp	28	90	60	80
18	Hydrocarbon oil + HAp	28	120	90	40

2.3. Experimentation

Out of total 18 experimental runs, nine were performed in pure medium i.e. hydrocarbon oil in ZNC-EDM (OSCARMAX, S645) dielectric tank itself whereas the following powder mixed trials were conducted in an in-house fabricated dielectric tank of capacity 12 liters. HAp was mixed at 15 g/l to the hydrocarbon oil and continuously circulated using a stirrer and pump to avoid the settling down of powder particles as shown in Fig. 1.

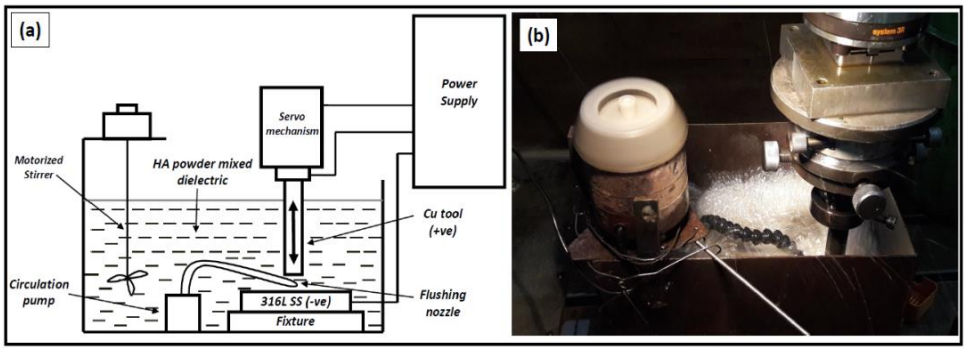

Fig. 1 (a) Schematic experimental setup and (b) indigenously developed dielectric tank

2.4. Investigation of machined samples

As it is evident from the previous studies [26-28] that biomaterial surface must be porous and must possess bioactive compounds to portray the bioactivity within the individual, the machined samples were investigated for porous microstructure, powder deposition and formation of new compounds using SEM and XRD analysis respectively.

Furthermore, Mitutoyo microhardness tester (Fig. 2) with diamond indenter was used to scrutinize the improved hardness of the ED machined specimens. A load of 0.98 N was

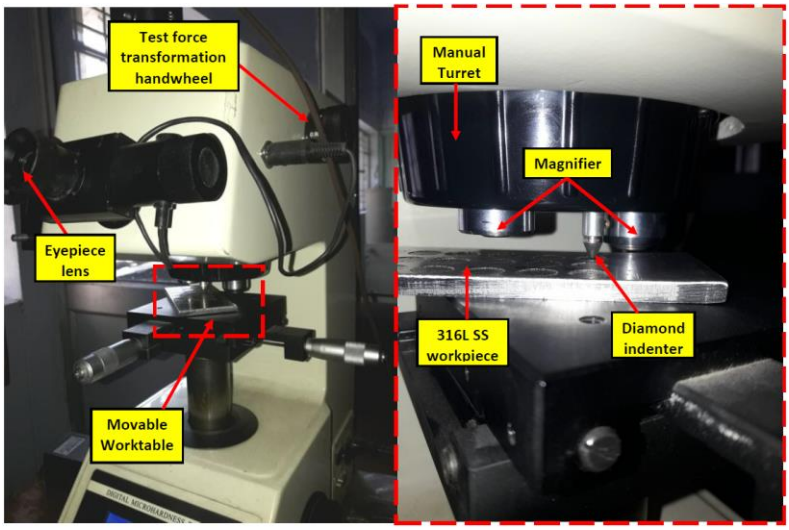

Fig. 2 Microhardness testing of ED machined samples

applied for a dwell time of 10 seconds to profile a pyramidal imprint on the specimen. Three readings were taken on each machined sample for both the plates and showed in Table 5 (Rep 1 for mean of plate 1 and Rep 2 for mean of plate 2). Prior to measurement, the microhardness of substrate was computed at three different points and an average value of 291.80 HV was noted.

3. Results and Discussion

Based upon the experimentation performed, the following Table 5 demonstrates the output response values and S/N ratios for both the workpiece plates. Further, the output responses were statistically analyzed through ANOVA to evaluate the percentage contribution of each input parameter and subsequently their rank.

Table 5 Response table for EDMed 316L stainless steel

Exp.	MRR (mg/min.)		S/N ratio	Microhardness (MH)		S/N ratio
Run	Rep 1	Rep 2	(MRR)	Rep 1	Rep 2	(MH)
1	2.81	2.53	8.4944	386.5	419.9	52.0881
2	4.65	4.01	12.6585	228.2	342.4	48.5804
3	4.84	6.50	14.7914	319.1	406.3	51.0022
4	10.02	10.63	20.2664	347.8	372.7	51.1165
5	5.21	6.12	14.9799	538.9	369.5	52.6890
6	6.32	5.68	15.5259	515.9	612.2	54.9313
7	11.50	11.61	21.2551	475.2	453.6	53.3308
8	13.16	8.84	20.3220	374.3	404.2	51.7853
9	6.44	8.21	17.1055	459.7	581.8	54.1531
10	6.23	6.42	16.0183	819.4	758.7	57.9228
11	4.15	7.19	14.1225	557.8	665.1	55.6268
12	4.36	4.97	13.3213	859.4	770.9	58.1863
13	10.64	8.98	19.7400	636.2	578.3	55.6377
14	10.86	7.13	18.5156	663.1	567.7	55.7048
15	5.31	4.03	13.1408	904.3	796.9	58.5425
16	17.49	20.52	25.4945	904.6	769.8	58.3720
17	6.98	5.67	15.8812	779.5	823.2	58.0668
18	11.80	12.86	21.7952	958.3	796.9	58.7556

(Rep 1 and Rep 2: repetitions of experimentations on two separate plates)

Digital weighing machine (Wensar, model: PGB 200) having least count of 0.001g was utilized for measuring the change in workpiece weight after each experimental run for evaluating the material removal rate of 316L SS using the following equation:

$$\text{MRR} = \frac{\text{Initial weight} - \text{Final weight}}{\text{Machining Time}} \times 1000 \,\text{mg/min.} \quad (1)$$

The hardness of biomaterial plays a key role during the cyclic loading on the implanted part particularly in the case of knee and hip joint. For that reason, the signal-to-noise (S/N ratios) analysis for microhardness as well as MRR was calculated according to equation (2) using Taguchi's criteria for larger-is-better for the current experimentation.

$$\left(\frac{S}{N}\right)_{LB} = -10\log\left\{\frac{1}{R}\sum_{i=1}^{R}\frac{1}{y_i^2}\right\} \tag{2}$$

where R is the repetition of responses and y_i the value of response at i^{th} trial.

3.1. Analysis of Material Removal Rate

Evaluation of MRR is a primary output response during the ED machining of the workpiece material. Minitab-17 was used to analyze the output values from Table 5 for both the workpiece plates in terms of signal-to-noise ratios and percentage contribution of input parameters. Fig. 3 and Table 6 illustrate the main effects plot for S/N ratios and analysis of variance (ANOVA) for MRR of current experimentation.

Superior material removal rate (19.01 mg/min.) was witnessed at higher value of peak current (28A) and pulse-on-time (120µs). Current depicts the highest percentage contribution of 52.66% followed by pulse-off (14.28%) and pulse-on (8.99%). Based on the responses, it is discovered that with an increase in the current intensity, the rate of material removal is sharply augmented and similar results can be observed from the S/N ratios plot.

Table 6 Analysis of variance for S/N ratios of MRR

Source	DF	Seq SS	Adj MS	F-value	p-value	% Contribution
Dielectric medium (Dm)	1	8.862	8.862	1.27	0.292	3.10
Ip (A)	2	150.409	75.205	10.81	0.005*	52.66
P-on (µs)	2	25.686	12.843	1.85	0.219	8.99
P-off (µs)	2	40.784	20.392	2.93	0.111	14.28
Voltage	2	4.241	2.120	0.30	0.746	1.48
Residual Error	8	55.673	6.959			19.49
Total	17	285.656				100.00

*Most significant at 95% confidence level; Rank 1: current; Rank 2: pulse-off; Rank 3: pulse-on

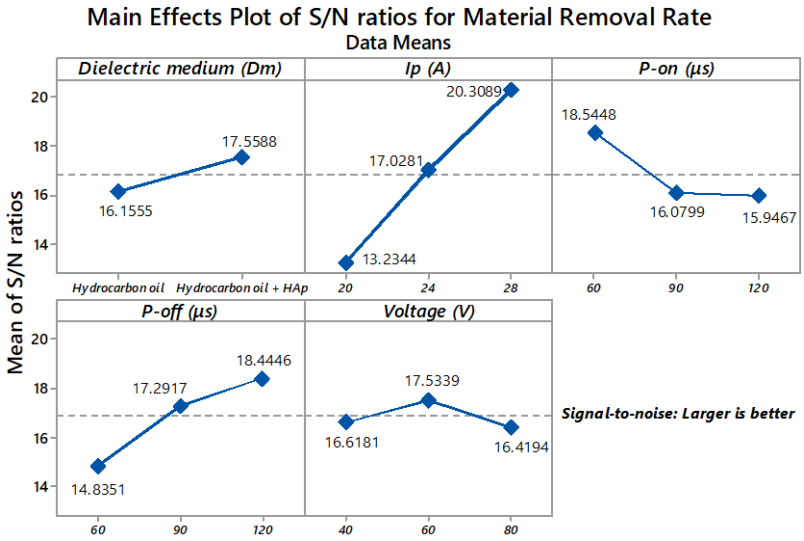

Fig. 3 S/N ratios plot for Material Removal Rate

3.2. Analysis of Microhardness

Analysis of variance was performed to check the dominance of hydroxyapatite powder and other chosen parameters; associated results for microhardness of EDMed 316L stainless steel surface are shown in Table 7. Superior microhardness of 877.60 HV is illustrated at the utmost values of current intensity (28A) and pulse-on-time (120µs) in the presence of HAp mixed dielectric (trial 18) with an increment of 79% and 160% comparative to the samples machined in hydrocarbon oil and substrate material, respectively.

At a higher value of discharge current and pulse-on, the spark generation between tool and workpiece acts more rapidly permitting the deposition of HA powder mixed in the dielectric medium. The breakdown of electrolyte (hydrocarbon oil) also formed intermetallic compounds reacting with substrate elements and facilitates improved hardness. Similar results can be observed from Fig. 4 and Table 7, dielectric medium (% contribution: 74.06%) portray as the most prominent factor directly influencing the microhardness of ED machined 316L SS surface.

Table 7 Analysis of variance for S/N ratios of Microhardness

Source	DF	Seq SS	Adj MS	F-value	p-value	% Contribution
Dielectric medium (Dm)	1	123.447	123.447	59.38	0.000*	74.06
Ip (A)	2	10.199	5.100	2.45	0.148	6.12
P-on (µs)	2	14.373	7.186	3.46	0.083	8.63
P-off (µs)	2	0.683	0.341	0.16	0.851	0.41
Voltage	2	1.341	0.670	0.32	0.733	0.80
Residual Error	8	16.633	2.079			9.98
Total	17	166.675				100.00

*Most significant at 95% confidence level; Rank 1: dielectric; Rank 2: pulse-on; Rank 3: current

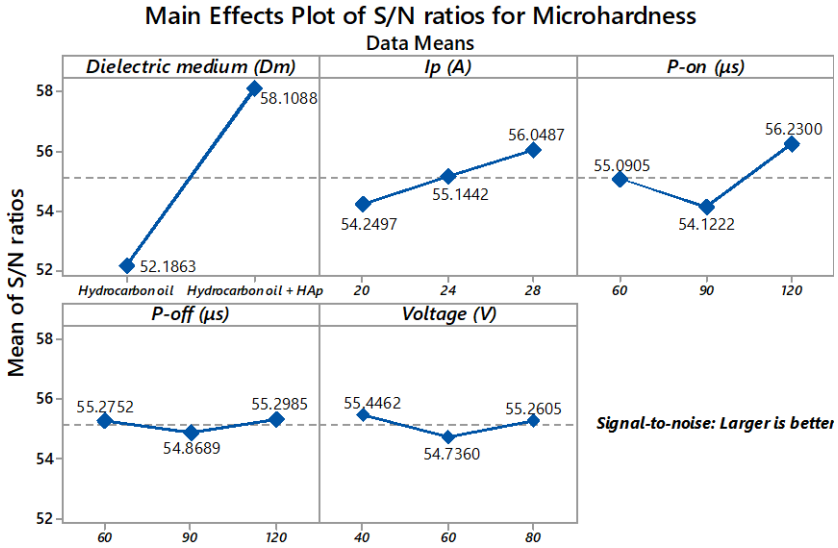

Fig. 4 S/N ratios plot for Microhardness

3.3. Surface evaluation of HA-PMEDMed 316L stainless steel

The machined surface with maximum value of microhardness (trial 18) was further examined for porous structure and deposition of powder particles through scanning electron microscopy. Fig. 6 (b) showed the microstructure of HA powder mixed dielectric depicting porosity in conjunction with surface modification of the substrate surface and deposition of powder particles. Apart from this, sample exhibiting maximum hardness (trial 8) in pure dielectric medium was also examined using SEM (Fig. 6a) and illustrates the cracks, craters on its surface.

The modified 316L stainless steel surface in HA powder mixed EDM was then analyzed for the changed elemental composition using XRD technique. Fig. 5 demonstrating the XRD pattern with the existence of various bioactive (calcium, phosphorus, calcium carbonate) and intermetallic (manganese silicide, chromium carbide, manganese silicide carbide) compounds on the HA-PMEDMed surface. As a result, modified surface not only restrict the fluidic reactions but also promotes the bioactivity offering better cell proliferation, biological fixation, etc. [29, 30].

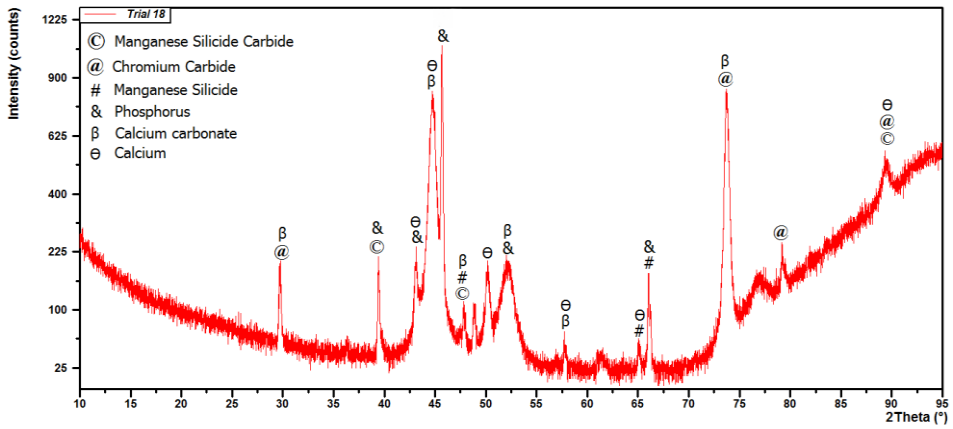

Fig. 5 XRD pattern for HA-PMEDMed surface (trial 18)

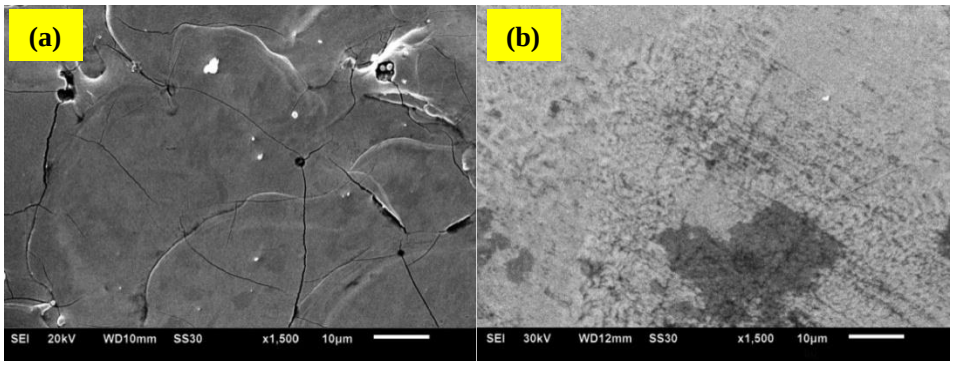

Fig. 6 SEM for maximum microhardness (a) machined in pure dielectric (trial 8); (b) porous surface with white powder layer (trial 18)

4. CONCLUSIONS

The current research work is an investigation of medical grade 316L stainless steel for the surface modification with hydroxyapatite powder mixed dielectric using reverse polarity of EDM. Based upon the experimental observation, the following conclusions are drawn:

- HAp powder mixed dielectric is the most influential factor affecting the microhardness (877.60 HV) with an augmentation of 160% and 79% comparative to substrate material and sample machined in pure dielectric.
- HA-PMEDMed surface testifies the presence of bioactive compounds and porous structure along with the presence of powder particles on the surface in XRD and SEM analysis respectively.
- Superior value of MRR (19.01 mg/min.) with current as momentous factor (contribution: 54.66%) is at Ip 28A, P-on 60µs, P-off 120µs and voltage 60V in the present of HAp mixed dielectric medium.

REFERENCES

1. Mahajan, A., Sidhu, S.S., 2017, *Surface modification of metallic biomaterials for enhanced functionality: A Review*, Materials Technology, 33(2), pp. 93-105.
2. Nagarajan, S., Rajendran, N., 2009, *Sol–gel derived porous zirconium dioxide coated on 316L SS for orthopedic applications*, Journal of Sol-Gel Science and Technology, 52(2), pp. 188-196.
3. Feng, K., Cai, X., Li, Z., Chu, P.K., 2012, *Improved corrosion resistance of stainless steel 316L by Ti ion implantation*, Materials Letters, 68, pp. 450-452.
4. Sharifnabi, A., Fathi, M.H., Eftekhari-Yekta, B., Hossainalipour, M., 2014, *The structural and bio-corrosion barrier performance of Mg-substituted fluorapatite coating on 316L stainless steel human body implant*, Applied Surface Science, 288, pp. 331-340.
5. Wang, L., Zhao, X., Ding, M.H., Zheng, H., Zhang, H.S., Zhang, B.L., Wu, G.Y., 2015, *Surface modification of biomedical AISI 316L stainless steel with zirconium carbonitride coatings*, Applied Surface Science, 340, pp. 113-119.
6. Manam, N.S., Harun, W.S.W., Shri, D.N.A., Ghani, S.A.C., Kurniawan, T., Ismail, M.H., Ibrahim, M.H.I., 2017, *Study of corrosion in biocompatible metals for implants: A review*, Journal of Alloys and Compounds, 701, pp. 698-715.
7. Uwais, Z.A., Hussein, M.A., Samad, M.A., Al-Aqeeli, N., 2017, *Surface modification of metallic biomaterials for better tribological properties: A review*, Arabian Journal of Science and Engineering, 42(11), pp. 4493-4512.
8. Harcuba, P., Bacakova, L., Strasky, J., Bacakova, M., Novotna, K., Janecek, M., 2012, *Surface treatment by electric discharge machining of Ti–6Al–4V alloy for potential application in orthopaedics*, Journal of the mechanical behaviour of biomedical materials, 7, pp. 96-105.
9. Mahajan, A., Sidhu, S.S., 2019, *In vitro corrosion and hemocompatibility evaluation of electrical discharge treated cobalt-chromium implant*, Journal of Materials Research, 34(8), pp. 1363-1370.
10. Singh, G., Sidhu, S.S., Bains, P.S., Bhui, A.S., 2019, *Surface evaluation of ED machined 316L stainless steel in TiO_2 nano-powder mixed dielectric medium*, Materials Today: Proceedings, 18(3), pp. 1297-1303.
11. Bains, P.S., Sidhu, S.S., Payal, H.S., Kaur, S., 2019, *Magnetic Field Influence on Surface Modifications in Powder Mixed EDM*, Silicon, 11(1), pp. 415-423.
12. Hubler, R., Cozza, A., Marcondes, T.L., Souza, R.B., Fiori, F.F., 2001, *Wear and corrosion protection of 316-L femoral implants by deposition of thin films*, Surface and Coatings Technology, 142-144, pp. 1078-1083.
13. Kumar, A.M., Rajendran, N., 2013, *Electrochemical aspects and in vitro biocompatibility of polypyrrole/TiO_2 ceramic nanocomposite coatings on 316L SS for orthopedic implants*, Ceramics International, 39(5), pp. 5639-5650.
14. Singh, G., Sidhu, S.S., Bains, P.S., Bhui, A.S., 2019, *Improving microhardness and wear resistance of 316L by TiO_2 powder electo-discharge treatment*, Materials Research Express, 6(8), 086501.
15. Chang, S.H., Chen, J.Z., Hsiao, S.H., Lin, G.W., 2014, *Nanohardness, corrosion and protein adsorption properties of CuAlO2 films deposited on 316L stainless steel for biomedical applications*, Applied Surface Science, 289, pp. 455-461.

16. Bhui, A.S., Singh, G., Sidhu, S.S., Bains, P.S., 2018, *Experimental investigation of optimal ED machining parameters for Ti-6Al-4V biomaterial*, Facta Universitatis-Series Mechanical Engineering, 16(3), pp. 337-345.
17. Harun, W.S.W., Asri, R.I.M., Alias, J., Zulkifli, F.H., Kadirgama, K., Ghani, S.A.C., Shariffuddin, J.H.M., 2018, *A comprehensive review of hydroxyapatite-based coatings adhesion on metallic biomaterials*, Ceramics International, 44(2), pp. 1250-1268.
18. Hameed, P., Gopal, V., Bjorklund, S., Ganvir, A., Sen, D., Markocsan, N., Manivasagam, G., 2019, *Axial suspension plasma spraying: An ultimate technique to tailor Ti6Al4V surface with HAp for orthopaedic applications*, Colloids and Surfaces B: Biointerfaces, 173, pp. 806-815.
19. Ananth, K.P., Sun, J., Bai, J., 2018, *Superior corrosion protection and in vitro biocompatibility of Na-HAp/CS composite coating on PoPD-coated 316L SS*, Materialstoday chemistry, 10, pp. 153-166.
20. Lamichhane, Y., Singh, G., Bhui, A.S., Mukhiya, P., Kumar, P., Thapa, B., 2019, *Surface modification of 316L SS with HAp nano-particles using PMEDM for enhanced biocompatibility*, Materials Today: Proceedings, 15(2), pp. 336-343.
21. Prakash, C., Kansal, H.K., Pabla, B.S., Puri, S., Aggarwal, A., 2015, *Electric discharge machining-A potential choice for surface modification of metallic implants for orthopedic applications: A review*, Proceedings of the Institution of Mechanical Engineers, Part B: Journal of Engineering Manufacture, 230(2), pp. 331-353.
22. Kumar, S., Singh, R., Singh, T.P., Sethi, B. L., 2009, *Surface modification by electrical discharge machining: A review*, Journal of Materials Processing Technology, 209(8), pp. 3675-3687.
23. Bains, P.S., Sidhu, S.S., Payal, H.S., 2018, *Magnetic field assisted EDM: New horizons for improved surface properties*, Silicon, 10(4), pp. 1275-1282.
24. Kumar, A., Maheshwari, S., Sharma, C., Beri, N., 2011, *Analysis of machining characteristics in additive mixed electric discharge machining of nickel-based super alloy Inconel 718*, Materials and Manufacturing Processes, 26(8), pp. 1011-1018.
25. Bhui, A.S., Bains, P.S., Sidhu, S.S., Singh, G., 2019, *Parametric optimization of ED machining of Ti-6Al-4V in CNTs mixed dielectric medium*, Materials Today: Proceedings, 18(3), pp. 1532-1539.
26. Subramanian, B., Ananthakumar, R., Kobayashi, A., Jayachandran, M., 2011, *Surface modification of 316L stainless steel with magnetron sputtered TiN/VN nanoscale multilayers for bio implant applications*, Journal of Materials Science: Materials in Medicine, 23(2), pp. 329-338.
27. Huang, Q., Yang, Y., Hu, R., Lin, C., Sun, L., Vogler, E.A., 2015, *Reduced platelet adhesion and improved corrosion resistance of superhydrophobic TiO_2-nanotube-coated 316L stainless steel*, Colloids and Surfaces B: Biointerfaces, 125, pp. 134-141.
28. Chen, Y., Frith, J.E., Dehghan-Manshadi, A., Attar, H., Kent, D., Soro, N.D.M., Bermingham, M.J., Dargusch, M.S., 2017, *Mechanical properties and biocompatibility of porous titanium scaffolds for bone tissue engineering*, Journal of the Mechanical Behavior of Biomedical Materials, 75, pp. 169-174.
29. Wang, L., Zhao, X., Ding, M.H., Zheng, H., Zhang, H.S., Zhang, B., Li, X.Q., Wu, G.Y., 2015, *Surface modification of biomaterial AISI 316L stainless steel with zirconium carbonitride coatings*, Applied Surface Science, 340, pp. 113-119.
30. Kaliaraj, G.S., Kumar, N., 2018, *Oxynitrides decorated 316L SS for potential bioimplant application*, Materials Research Express, 5(3), 036403.